Featured in Physics

Phonon Thermal Hall Conductivity from Scattering with Collective Fluctuations

Léo Mangeolle,[1] Leon Balents,[2,3] and Lucile Savary[1,2]

[1]*École Normale Supérieure de Lyon, CNRS, Laboratoire de physique, 46, allée d'Italie, 69007 Lyon*
[2]*Kavli Institute for Theoretical Physics, University of California, Santa Barbara, California 93106-4030, USA*
[3]*Canadian Institute for Advanced Research, Toronto ON M5G 1M1, Ontario, Canada*

(Received 21 February 2022; revised 3 July 2022; accepted 26 September 2022; published 21 December 2022)

Because electrons and ions form a coupled system, it is *a priori* clear that the dynamics of the lattice should reflect symmetry breaking within the electronic degrees of freedom. Recently, this has been clearly evidenced for the case of time-reversal and mirror symmetry breaking by observations of a large phononic thermal Hall effect in many strongly correlated electronic materials. However, the mechanism by which time-reversal breaking and chirality is communicated to the lattice is far from evident. In this paper, we discuss how this occurs via many-body scattering of phonons by collective modes: a consequence of non-Gaussian correlations of the latter modes. We derive fundamental new results for such skew (i.e., chiral) scattering and the consequent thermal Hall conductivity. We emphasize that these results apply to any collective variables in any phase of matter: electronic, magnetic, or neither; highly fluctuating and correlated, or not. As a proof of principle, we compute general formulas for the above quantities for ordered antiferromagnets. From the latter, we obtain the scaling behavior of the phonon thermal Hall effect in clean antiferromagnets. The calculations show several different regimes and give quantitative estimates of similar order to that seen in recent experiments.

DOI: 10.1103/PhysRevX.12.041031

Subject Areas: Condensed Matter Physics, Magnetism, Strongly Correlated Materials

I. INTRODUCTION

Thermal conductivity is the most ubiquitous transport coefficient, being well defined in any system with sufficiently local interactions, irrespective of the nature of the specific low-energy degrees of freedom. Therefore, it is particularly important in systems for which charge transport is either strongly suppressed (i.e., insulators) or singular (i.e., superconductors). Moreover, the thermal Hall conductivity plays a particularly special role in the theory of exotic topological phases, as it can be related to the chiral central charge, to the presence of edge modes, etc. For all of the above reasons, experiments on thermal conductivity have played a preeminent role in establishing the nature of the most interesting strongly correlated states of matter. A few notable examples are the observation of metalliclike transport in an organic spin liquid [1], a quantized thermal Hall effect in the Kitaev material α-$RuCl_3$ [2] (taken as evidence for Majorana fermion edge states), and an exceptionally large and yet unexplained thermal Hall effect in underdoped cuprate high-temperature superconducting materials [3,4].

Arguably, the Achilles heel of thermal conductivity measurements is the contribution of lattice vibrations or phonons to heat transport. Phonons are present in any solid, and indeed, except at very low temperatures, usually dominate the thermal properties of materials. A common approach is to attempt to separate electronic and lattice contributions by some subtraction scheme, for example, based on measuring two electronically different but vibrationally similar analog materials, or on the dependence on temperature, field, etc., which might be attributed uniquely to only one of the lattice or electronic degrees of freedom. Of particular significance in this regard is the thermal Hall effect, which, by Onsager relations, can only exist when time-reversal symmetry is broken [5]. The Hall conductivity is captured by the antisymmetric components of the thermal conductivity tensor $\boldsymbol{\kappa}$, namely,

$$\kappa_H^{\mu\nu}(T, \boldsymbol{H}, \cdots) = (\kappa^{\mu\nu} - \kappa^{\nu\mu})/2. \tag{1}$$

It is often assumed that the charge neutrality of phonons and the large ionic mass are sufficient to prevent them from coupling effectively to internal or external magnetic fields and, therefore, that large thermal Hall signals must arise uniquely from the electrons in a material. Many recent

theoretical works have thus focused on the thermal Hall conductivity of spin excitations [6–10], in particular, spin waves [11–14].

However, recent experiments have conclusively shown that this assumption is incorrect, via the simplest and most persuasive of arguments [15–17]. In particular, studies of materials that are electronically (or magnetically) two dimensional have observed that the thermal Hall conductivity is three dimensional and remains large when the thermal current within the sample is normal to the two-dimensional planes [18]. One has no choice but to conclude that the transported heat is carried by phonons.

The problem posed by these observations is then to understand how lattice vibrations "sense" time-reversal symmetry breaking. This must indeed be by an indirect process, as ultimately it is the electrons that interact directly and significantly with magnetic fields. In principle, there are two broad ways in which the transfer of information, i.e., the breaking of time-reversal symmetry, can occur from electrons to the lattice. First, it can occur via the quasi-adiabatic adaptation of electronic states to slow phonon motions, which may modify the phonon dispersion relations and generate dynamical Berry phases [19–22]. While this is certainly possible in principle, numerous estimates indicate that this mechanism is unlikely to explain the large magnitude of thermal Hall signals seen in experiments. The second type of information transfer, depicted in Fig. 1, is through scattering of phonons from the electronic modes, which can be "chiral" when the latter break time-reversal and reflection symmetries. In the electrical anomalous Hall effect, such "skew scattering" is known to dominate in the most highly conducting samples [23], and for similar reasons, we expect it to do so for heat transport when thermal conductivity is large.

With this in mind, it is critical to ask how time-reversal symmetry breaking of electronic degrees of freedom is communicated *via scattering* to phonons in clean systems. We assume perturbative coupling of some set of collective fields Q to the lattice, which is generally valid away from the limit of polaron formation [24,25]. To account for the diversity of different electronic and magnetic phases being studied, we allow the fields Q to be *general*, restricted only by the requirements of unitarity of quantum mechanics and equilibrium. We show that the full scattering data needed to understand the thermal conductivity (both longitudinal and Hall components) can be obtained from the time- and space-dependent correlation functions of the Q fields. Crucially, we show that the standard two-point correlation functions of Q give vanishing contributions to skew scattering and the Hall effect. Consequently, the skew scattering can be attributed entirely to non-Gaussian fluctuations of the collective modes. This is a challenge theoretically (because as we discuss below, beyond-Gaussian fluctuations are significantly more complex than Gaussian ones) but also an opportunity. The absence of lower-order contributions to skew scattering means that the latter provides a direct probe of non-Gaussianity, which does not require any subtraction. This suggests the prospect of using measures of skew scattering of phonons, such as the thermal Hall effect, as a means to interrogate the rich higher-order correlations of electronic modes.

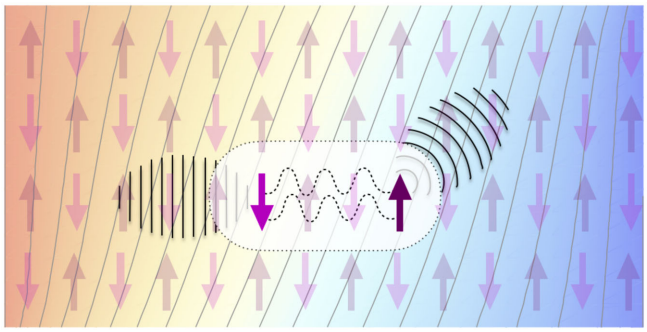

FIG. 1. Illustration of a scattering mechanism responsible for a Hall effect. Only scattering processes that involve at least two (virtual) collisions with collective fluctuations can contribute to a Hall effect.

In this paper, we identify the corresponding higher-order correlation functions that relate the multiphonon scattering rates to the fluctuations of the collective modes. These are complicated objects that depend upon several time and space coordinates or, equivalently, multiple frequencies and wave vectors. We show how to extract the essentially antisymmetric part of these correlations that uniquely contribute to the Hall effect, using symmetry and detailed balance relations, which generalize well-known and ubiquitously important laws that are used to analyze two-point correlations throughout physics [26–28]. This provides a recipe that can be applied in diverse systems, telling what is known about the electronic modes coupled to the lattice and how to use those data to obtain an understanding of the thermal Hall effect of phonons. Notably, the results are valid irrespective of the nature of the phase of matter hosting the collective fields: It may be strongly fluctuating, highly correlated, or even have no quasiparticles at all. This contrasts greatly with prior theories of phonon skew scattering that are based on very specific models of electronic modes [29,30].

To demonstrate the methodology and as a proof of principle, we also apply the general results to the case of an ordered antiferromagnet, in which case the Q fields correspond to magnetic fluctuations that can be decomposed into composites of magnons. The result is a richly structured skew-scattering rate, visualized in Fig. 2. Validating the general formulation, we obtain a nonvanishing thermal Hall effect when all the symmetry criteria (which we establish) are satisfied, and we explicitly show that within a minimal model of an antiferromagnet with strictly two-dimensional magnetic correlations, the thermal Hall effect is three dimensional and its magnitude is

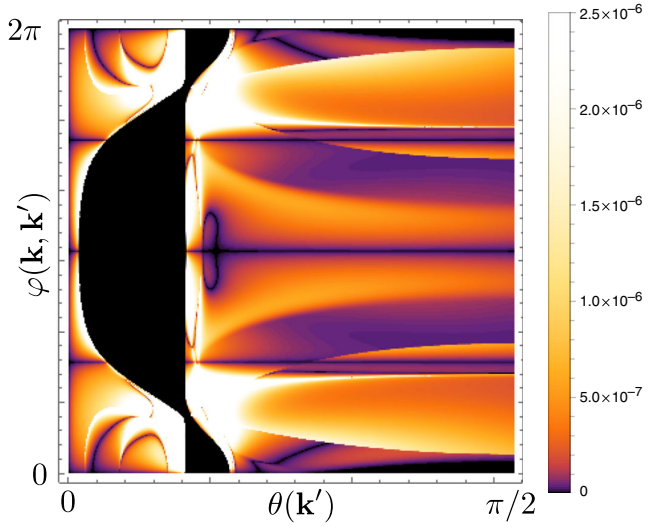

FIG. 2. Calculated skew-scattering rate $\mathfrak{W}^{\ominus,-+}_{n\mathbf{k}n'\mathbf{k}'}/\gamma_0$ [see Eqs. (10) and (19)] to transfer a phonon in mode $n'\mathbf{k}'$ to mode $n\mathbf{k}$, induced by coupling the lattice to a two-dimensional antiferromagnet. The density plot shows the angular dependence as a function of $\theta(\mathbf{k}') \in [0, \pi/2]$ (horizontal axis) and $\varphi(\mathbf{k}, \mathbf{k}') = \phi(\mathbf{k}') - \phi(\mathbf{k})$ (vertical axis) for fixed $|\mathbf{k}'| = 0.8/\mathfrak{a}$, $k_x = 0.2/\mathfrak{a}$, $k_y = 0$, $k_z = 0.1/\mathfrak{a}$, $\boldsymbol{m}_0 = 0.05\hat{z}$, and temperature $T = 0.5T_0$. Here, $\mathfrak{a}$ is the in-layer lattice spacing, and $\phi(\mathbf{k}^{(\prime)})$ and $\theta(\mathbf{k}^{(\prime)})$ are the azimuthal and polar angles of $\mathbf{k}^{(\prime)}$, defined in the usual way. Note that the color bar is not scaled linearly.

roughly independent of whether the thermal currents are within or normal to the magnetic planes.

II. SCATTERING AND CORRELATION FUNCTIONS

In this section, we present the main results for the scattering rates of phonons due to collective modes. We limit the discussion here to the simplest case in which the coupling is linear in phonon creation or annihilation operators $a^\dagger_{n\mathbf{k}}, a_{n\mathbf{k}}$. Then, the coupling Hamiltonian is

$$H' = \sum_{n\mathbf{k}} (a^\dagger_{n\mathbf{k}} Q^\dagger_{n\mathbf{k}} + a_{n\mathbf{k}} Q_{n\mathbf{k}}), \tag{2}$$

where $Q_{n\mathbf{k}}$ describes the collective mode arising from electronic degrees of freedom, coupled to the nth phonon polarization. For brevity, we subsume any electron-phonon coupling constant into $Q_{n\mathbf{k}}$. We carry out a perturbative analysis of H', so $Q_{n\mathbf{k}}$ may be regarded as "small."

A. Formulation

Our aim is to calculate the necessary terms in the collision integral $\mathcal{C}_{n\mathbf{k}}$ of the phonon Boltzmann equation,

$$\partial_t \bar{N}_{n\mathbf{k}} + \boldsymbol{v}_{n\mathbf{k}} \cdot \boldsymbol{\nabla}_{\mathbf{r}} \bar{N}_{n\mathbf{k}} = \mathcal{C}_{n\mathbf{k}}[\{\bar{N}_{n'\mathbf{k}'}\}], \tag{3}$$

where $\bar{N}_{n\mathbf{k}}$ is the nonequilibrium average occupation number of phonons in polarization mode n and quasimomentum $\mathbf{k}$ with velocity $\boldsymbol{v}_{n\mathbf{k}} = \boldsymbol{\nabla}_{\mathbf{k}} \omega_{n\mathbf{k}}$, where $\omega_{n\mathbf{k}}$ is the $(n, \mathbf{k})$ phonon dispersion relation. Once the collision integral is known, the Boltzmann equation can be solved in a standard manner by linearizing around the equilibrium distribution to obtain the nonequilibrium change and thereby the transport current to linear order in the temperature gradient.

We now summarize the method used to obtain the collision integral from the microscopic quantum dynamics and Eq. (2). The basic procedure is to determine the many-body transition rate between microstates in the combined phonon-electron system using the scattering matrix (T) expansion and, from there, use the equilibrium distribution for the electronic subsystem to evaluate the rate of change of the mean occupation probabilities of phonon states that enter the Boltzmann equation.

We begin with the Born expansion [31]:

$$T_{\mathtt{i}\to\mathtt{f}} = T_{\mathtt{fi}} = \langle \mathtt{f}|H'|\mathtt{i}\rangle + \sum_{\mathtt{n}} \frac{\langle \mathtt{f}|H'|\mathtt{n}\rangle\langle \mathtt{n}|H'|\mathtt{i}\rangle}{E_{\mathtt{i}} - E_{\mathtt{n}} + i\eta} + \cdots, \tag{4}$$

where the $|\mathtt{i}\rangle, |\mathtt{f}\rangle, |\mathtt{n}\rangle$ states are product states in the Q (index s) and phonon (index p) Hilbert space; $|\mathtt{g}\rangle = |g_s\rangle|g_p\rangle$ for $g = i, f, n$; and $E_{\mathtt{g}}$ is the energy of the unperturbed Hamiltonians of the Q and phonons in state $\mathtt{g}$. Here, $\eta \to 0^+$ is a small regularization parameter.

The rate of transitions from state $\mathtt{i}$ to state $\mathtt{f}$ is obtained using Fermi's golden rule,

$$\Gamma_{\mathtt{i}\to\mathtt{f}} = \frac{2\pi}{\hbar} |T_{\mathtt{i}\to\mathtt{f}}|^2 \delta(E_{\mathtt{i}} - E_{\mathtt{f}}). \tag{5}$$

Note that $\Gamma_{\mathtt{i}\to\mathtt{f}}$ is a transition rate in the full combined phonon-Q system. By assuming equilibrium for the electronic modes, we obtain the transition rates within the phonon subsystem,

$$\tilde{\Gamma}_{i_p \to f_p} = \sum_{i_s f_s} \Gamma_{\mathtt{i}\to\mathtt{f}} p_{i_s}, \tag{6}$$

with $p_{i_s} = (1/Z_s) e^{-\beta E_{i_s}}$. This in turn determines the collision integral through the master equation

$$\mathcal{C}_{n\mathbf{k}} = \sum_{i_p, f_p} \tilde{\Gamma}_{i_p \to f_p} (N_{n\mathbf{k}}(f_p) - N_{n\mathbf{k}}(i_p)) p_{i_p}, \tag{7}$$

where $p_{i_p} = \sum_{i_s} p_{\mathtt{i}}$, with $p_{\mathtt{i}}$ the probability to find the system in state $\mathtt{i}$.

B. Result

To carry out the above procedure, we first express the microscopic processes generated in the Born expansion, Eq. (4), and insert them into the square in Eq. (5). Then, the sums over electronic states i_s, f_s in Eq. (6) can be converted into dynamical multitime correlation functions of the Q

operators. The corresponding technical manipulations are described in Appendix A. The leading result for the longitudinal conductivity [symmetric part of the tensor, $\kappa_L^{\mu\nu} = (\kappa^{\mu\nu} + \kappa^{\nu\mu})/2$] is dominated by diagonal scattering (absorption or emission of a single phonon), and it is given by

$$\kappa_L^{\mu\nu} = \frac{\hbar^2}{k_B T^2} \frac{1}{V} \sum_{n\mathbf{k}} \frac{\omega_{n\mathbf{k}}^2 v_{n\mathbf{k}}^\mu v_{n\mathbf{k}}^\nu}{4 D_{n\mathbf{k}} \sinh^2(\beta\hbar\omega_{n\mathbf{k}}/2)}, \tag{8}$$

where V is the volume of the system; $\mu, \nu = x, y, z$; and $D_{n\mathbf{k}}$ is the longitudinal scattering rate [see Eq. (11)]. For the Hall effect, the important contributions are those from the second-order terms in the Born expansion, which generate processes in which a phonon is scattered from one state to another, or in which pairs of phonons are created or annihilated. Using Eq. (7) then leads to off-diagonal terms in the collision integral, i.e., contributions to $\mathcal{C}_{n\mathbf{k}}$ proportional to $N_{n'\mathbf{k}'}$, with $n'\mathbf{k}' \neq n\mathbf{k}$. The desired "skew" scattering contributions, roughly speaking, correspond to processes in which $\mathbf{k}$ is preferentially deflected "to the right" of $\mathbf{k}'$, for example.

More precisely, we define antisymmetric scattering rates $\mathfrak{W}^{\ominus,+,q}_{n\mathbf{k},n'\mathbf{k}'}$ $(q = \pm)$ in such a way that they control the antisymmetric (Hall) part of the thermal conductivity tensor, $\kappa_H^{\mu\nu} = -\kappa_H^{\nu\mu}$:

$$\kappa_H^{\mu\nu} = \frac{\hbar^2}{k_B T^2} \frac{1}{V} \sum_{n\mathbf{k}n'\mathbf{k}'} J_{n\mathbf{k}}^\mu \frac{e^{\beta\hbar\omega_{n\mathbf{k}}/2}}{2D_{n\mathbf{k}}} \left(\frac{1}{N_{\mathrm{uc}}} \sum_{q=\pm} \frac{(e^{\beta\hbar\omega_{n\mathbf{k}}} - e^{q\beta\hbar\omega_{n'\mathbf{k}'}}) \mathfrak{W}^{\ominus,+,q}_{n\mathbf{k},n'\mathbf{k}'}}{\sinh(\beta\hbar\omega_{n\mathbf{k}}/2) \sinh(\beta\hbar\omega_{n'\mathbf{k}'}/2)} \right) \frac{e^{\beta\hbar\omega_{n'\mathbf{k}'}/2}}{2D_{n'\mathbf{k}'}} J_{n'\mathbf{k}'}^\nu, \tag{9}$$

where, for $q, q' = \pm 1$,

$$\mathfrak{W}^{\ominus,qq'}_{n\mathbf{k}n'\mathbf{k}'} = \frac{2N_{\mathrm{uc}}}{\hbar^4} \mathfrak{Re} \int_{t,t_1,t_2} e^{i[\Sigma^{q,q'}_{n\mathbf{k}n'\mathbf{k}'} t + \Delta^{q,q'}_{n\mathbf{k}n'\mathbf{k}'}(t_1+t_2)]} \mathrm{sign}(t_2) \langle [Q^{-q}_{n\mathbf{k}}(-t-t_2), Q^{-q'}_{n'\mathbf{k}'}(-t+t_2)] \{ Q^{q'}_{n'\mathbf{k}'}(-t_1), Q^{q}_{n\mathbf{k}}(t_1) \} \rangle \tag{10}$$

and

$$D_{n\mathbf{k}} = -\frac{1}{\hbar^2} \int dt e^{-i\omega_{n\mathbf{k}} t} \langle [Q_{n\mathbf{k}}(t), Q^\dagger_{n\mathbf{k}}(0)] \rangle_\beta + \check{D}_{n\mathbf{k}}. \tag{11}$$

Here, $\langle \cdots \rangle_\beta$ denotes the expectation value at inverse temperature β, and $\mu, \nu = x, y, z$; we define the phonon current $J_{n\mathbf{k}}^\mu = N_{n\mathbf{k}}^{\mathrm{eq}} \omega_{n\mathbf{k}} v_{n\mathbf{k}}^\mu$, and $N_{n\mathbf{k}}^{\mathrm{eq}}$ is the number of phonons in mode $n\mathbf{k}$ in thermal equilibrium. Equation (11) gives the leading-order result for the diagonal scattering rate $D_{n\mathbf{k}}$, which enters Eq. (9). In general, it includes contributions $\check{D}_{n\mathbf{k}}$ from other scattering channels (e.g., impurities) and higher-order contributions. In Eq. (10), we introduced the notation $Q^+_{n\mathbf{k}} = Q^\dagger_{n\mathbf{k}}$ and $Q^-_{n\mathbf{k}} = Q_{n\mathbf{k}}$, as well as $\Sigma^{q,q'}_{n\mathbf{k}n'\mathbf{k}'} = q\omega_{n\mathbf{k}} + q'\omega_{n'\mathbf{k}'}$ and $\Delta^{q,q'}_{n\mathbf{k}n'\mathbf{k}'} = q\omega_{n\mathbf{k}} - q'\omega_{n'\mathbf{k}'}$. Here and in the following, lower case latin q (with or without primes or subscripts) is used to indicate a particle-hole index taking values $\pm 1 = \pm$.

Equations (9) and (10) constitute the central result of this paper. They give a general formula for the skew-scattering rate and the thermal Hall conductivity, given in Eq. (2), assuming a small Hall angle (a condition which is nearly always true), valid in any dimension. Even more general formulas valid when electronic modes are coupled to both linear and quadratic functions of the phonons will be given in a separate publication [32]. These results can be applied to any material provided the non-Gaussian correlations of the collective degrees of freedom corresponding to $Q_{n\mathbf{k}}$ are known.

Considerable structure is encoded in Eq. (10). It is straightforward to show that the skew scattering vanishes if $Q_{n\mathbf{k}}$ is taken to be Gaussian: In this case, Wick's theorem is obeyed, and its application to Eq. (10) implies that $\mathfrak{W}^{\ominus}_{n\mathbf{k}n'\mathbf{k}'}$ is zero if $(n, \mathbf{k}) \neq (n', \mathbf{k}')$. Hence, nontrivial contributions to the skew scattering arise entirely from non-Gaussian correlations. Physically, $\mathfrak{W}^{\ominus,++}$ (respectively, $\mathfrak{W}^{\ominus,--}$) corresponds to scattering processes where two phonons are emitted (respectively, absorbed), and $\mathfrak{W}^{\ominus,+-}$, $\mathfrak{W}^{\ominus,-+}$ to processes where one phonon is emitted and one is absorbed. The contribution to the Hall conductivity has been carefully isolated so that the rate obeys the "anti-detailed balance" relation:

$$\mathfrak{W}^{\ominus,qq'}_{n\mathbf{k}n'\mathbf{k}'} = -e^{-\beta(q\omega_{n\mathbf{k}} + q'\omega_{n'\mathbf{k}'})} \mathfrak{W}^{\ominus,-q-q'}_{n\mathbf{k}n'\mathbf{k}'}, \tag{12}$$

as well as

$$\mathfrak{W}^{\ominus,qq'}_{n\mathbf{k}n'\mathbf{k}'} = \mathfrak{W}^{\ominus,q'q}_{n'\mathbf{k}'n\mathbf{k}}. \tag{13}$$

The combination of the commutator and anticommutator in Eq. (10) ensures the validity of these relations.

III. APPLICATION TO AN ORDERED ANTIFERROMAGNET

We now provide an application of the above results to the specific case of an insulating antiferromagnet. This is important as a proof of principle to confirm that the general

formula in Eq. (10) indeed results in a nonvanishing Hall effect of phonons from skew scattering. It is also a relevant test case as it corresponds to the situation in many recent experiments, and it is perhaps the simplest situation in which time-reversal symmetry breaking of spins is communicated to phonons in an insulator.

To model the antiferromagnet, we employ a spin-wave description and, for concreteness, assume the spin correlations are purely two dimensional: Each layer of spins is presumed to be completely independent. The latter assumption is not essential, but it is illustrative: Using it, we demonstrate that even when spin correlations are confined to two dimensions, their influence can lead to thermal Hall conductivity with heat current oriented perpendicular to those layers. In any case, the general formulas in the first subsection below can be easily modified for the case of three-dimensional spin waves.

A. Formulation and general results within linear spin-wave theory

The spin waves are described by magnon operators $b^\dagger_{\ell\mathbf{k},z}$ ($b_{\ell\mathbf{k},z}$), which create (annihilate) a magnon in branch ℓ with momentum $\mathbf{k}$ in layer $z \in \mathbb{N}$, whose Hamiltonian is

$$H_m = \sum_{\ell,\mathbf{k},z} \Omega_{\mathbf{k},\ell} b^\dagger_{\ell\mathbf{k},z} b_{\ell\mathbf{k},z}. \tag{14}$$

Note that the effect of a magnetic field is already included in H_m; i.e., here, the spin-wave modes are based on an expansion around the spin order *including* the effect of the field. The collective modes $Q^q_{n\mathbf{k}}$ can be expanded in a series in the spin-wave operators, and the dominant contribution to scattering comes from second order [33]:

$$Q^q_{n\mathbf{k}} = \frac{1}{\sqrt{N_{\mathrm{uc}}}} \sum_{\substack{\mathbf{p},\ell_1,\ell_2 \\ q_1,q_2,z}} \mathcal{B}^{n,\ell_1,\ell_2|q_1q_2q}_{\mathbf{k};\mathbf{p}} e^{ik_z z} b^{q_1}_{\ell_1,\mathbf{p}+\frac{q}{2}\mathbf{k},z} b^{q_2}_{\ell_2,-\mathbf{p}+\frac{q}{2}\mathbf{k},z}, \tag{15}$$

where $q = \pm 1$ and the sums run over $\mathbf{p}$ in the 2D Brillouin zone, and $q_{1,2} = \pm 1$, $z \in \mathbb{N}$, and $\ell_{1,2}$ over the magnon branches. Here, we define the notations

$$b^+_{\ell,\mathbf{p},z} = b^\dagger_{\ell,\mathbf{p},z}, \qquad b^-_{\ell,\mathbf{p},z} = b_{\ell,-\mathbf{p},z}. \tag{16}$$

Note the minus sign in the momentum in the second relation. Generally, this means that $(b^q_{\ell,\mathbf{p},z})^\dagger = b^{-q}_{\ell,-\mathbf{p},z}$. To make the coefficients unambiguous, we choose the symmetrized form $\mathcal{B}^{n,\ell_1,\ell_2|q_1q_2q}_{\mathbf{k};\mathbf{p}} = \mathcal{B}^{n,\ell_2,\ell_1|q_2q_1q}_{\mathbf{k};-\mathbf{p}}$. Demanding that $Q^+_{n\mathbf{k}} = (Q^-_{n\mathbf{k}})^\dagger$ implies that $\mathcal{B}^{n,\ell_1,\ell_2|q_1q_2+}_{\mathbf{k};\mathbf{p}} = (\mathcal{B}^{n,\ell_2,\ell_1|-q_2-q_1-}_{\mathbf{k};\mathbf{p}})^*$.

Equation (14) contains the energy dispersion $\Omega_{\mathbf{k},\ell}$ of the spin waves, but their wave functions are implicit. That information is encoded in the $\mathcal{B}$ coefficients. To obtain them, one should start with a microscopic spin-lattice coupling, expand it with Holstein-Primakoff bosons, and then use the canonical Bogoliubov transformation, which achieves the diagonal form of Eq. (14), to express the coupling as in Eq. (15). We apply this procedure to a particular case in Sec. III B. The following general results hold beyond this specific case and only assume Eqs. (14) and (15) as a starting point.

We proceed by evaluating Eqs. (9) and (11) and use Wick's theorem [valid for the free boson Hamiltonian in Eq. (14)] to compute the necessary correlation functions, decomposing them into products of the free-particle two-point function,

$$\langle b^{q_1}_{\ell_1,\mathbf{p}_1,z_1}(t_1) b^{q_2}_{\ell_2,\mathbf{p}_2,z_2}(t_2)\rangle = \delta_{\ell_1,\ell_2}\delta_{z_1,z_2}\delta_{q_1,-q_2}\delta_{\mathbf{p}_1+\mathbf{p}_2,0} \times f_{q_2}(\Omega_{\ell_1,q_1\mathbf{p}_1}) e^{-iq_2\Omega_{\ell_2,q_2\mathbf{p}_2}(t_1-t_2)}. \tag{17}$$

Here, $f_q(\Omega) = (1+q)/2 + n_{\mathrm{B}}(\Omega)$, where $n_{\mathrm{B}}(\Omega)$ is the Bose distribution.

This results in the following expressions for the diagonal and off-diagonal scattering rates:

$$D^{(s)}_{n\mathbf{k}} = \frac{(3-s)\pi}{\hbar^2 N^{\mathrm{2D}}_{\mathrm{uc}}} \sum_{\mathbf{p}} \sum_{\ell,\ell'} \frac{\sinh(\frac{\beta}{2}\hbar\omega_{n\mathbf{k}})}{\sinh(\frac{\beta}{2}\hbar\Omega^{\ell,+}_{\mathbf{p}}) \sinh(\frac{\beta}{2}\hbar\Omega^{\ell',-s}_{\mathbf{p}+\mathbf{k}})} \delta(\omega_{n\mathbf{k}} - \Omega^{\ell,+}_{\mathbf{p}} - s\Omega^{\ell',-s}_{\mathbf{p}+\mathbf{k}}) |\mathcal{B}^{n,\ell,\ell'|+s-}_{\mathbf{k};\mathbf{p}+\frac{\mathbf{k}}{2}}|^2, \tag{18}$$

where $s = \pm$ and $D_{n\mathbf{k}} = \sum_s D^{(s)}_{n\mathbf{k}} + \check{D}_{n\mathbf{k}}$. Here, we define $\Omega^{\ell,q}_{\mathbf{p}} = \Omega_{\ell,q\mathbf{p}}$, and for $q, q' = \pm 1$,

$$\mathfrak{W}^{\ominus,qq'}_{n\mathbf{k},n'\mathbf{k}'} = \frac{64\pi^2}{\hbar^4} \frac{1}{N^{\mathrm{2D}}_{\mathrm{uc}}} \sum_{\mathbf{p}} \sum_{\{\ell_i,q_i\}} \mathfrak{D}^{nn'|q_1q_2q_3,\ell_1\ell_2\ell_3}_{q\mathbf{k}q'\mathbf{k}',\mathbf{p}} \mathfrak{F}^{q_1q_2q_4,\ell_1\ell_2\ell_3}_{q\mathbf{k}q'\mathbf{k}',\mathbf{p}} \mathfrak{Im}\Big\{ \mathcal{B}^{n\ell_2\ell_3|q_2q_3q}_{\mathbf{k},\mathbf{p}+\frac{1}{2}q\mathbf{k}+q'\mathbf{k}'} \mathcal{B}^{n'\ell_3\ell_1|-q_3q_1q'}_{\mathbf{k}',\mathbf{p}+\frac{1}{2}q'\mathbf{k}'} \times \mathrm{PP}\Big[\frac{\mathcal{B}^{n\ell_1\ell_4|-q_1q_4-q}_{\mathbf{k},\mathbf{p}+\frac{1}{2}q\mathbf{k}} \mathcal{B}^{n'\ell_4\ell_2|-q_4-q_2-q'}_{\mathbf{k}',\mathbf{p}+q\mathbf{k}+\frac{1}{2}q'\mathbf{k}'}}{\Delta^{qq'}_{n\mathbf{k}n'\mathbf{k}'} + q_1\Omega^{\ell_1,-q_1}_{\mathbf{p}} - q_2\Omega^{\ell_2,q_2}_{\mathbf{p}+q\mathbf{k}+q'\mathbf{k}'} - 2q_4\Omega^{\ell_4,-q_4}_{\mathbf{p}+q\mathbf{k}}} + \frac{\mathcal{B}^{n'\ell_1\ell_4|-q_1-q_4-q'}_{\mathbf{k}',\mathbf{p}+\frac{1}{2}q'\mathbf{k}'} \mathcal{B}^{n\ell_4\ell_2|q_4-q_2-q}_{\mathbf{k},\mathbf{p}+\frac{1}{2}q\mathbf{k}+q'\mathbf{k}'}}{\Delta^{qq'}_{n\mathbf{k}n'\mathbf{k}'} - q_1\Omega^{\ell_1,-q_1}_{\mathbf{p}} + q_2\Omega^{\ell_2,q_2}_{\mathbf{p}+q\mathbf{k}+q'\mathbf{k}'} - 2q_4\Omega^{\ell_4,q_4}_{\mathbf{p}+q'\mathbf{k}'}} \Big] \Big\}, \tag{19}$$

where $\{\ell_i, q_i\} = \{\ell_1, \ell_2, \ell_3, \ell_4, q_1, q_2, q_3, q_4\}$, with $q_j = \pm 1$, and ℓ_j runs over the magnon branch indices. Here, we used, as before, $\Sigma^{q,q'}_{n\mathbf{k}n'\mathbf{k}'} = q\omega_{n\mathbf{k}} + q'\omega_{n'\mathbf{k}'}$, $\Delta^{q,q'}_{n\mathbf{k}n'\mathbf{k}'} = q\omega_{n\mathbf{k}} - q'\omega_{n'\mathbf{k}'}$, and we defined the product of delta functions $\mathfrak{D}$ and "thermal factor" $\mathfrak{F}$:

$$\begin{aligned}\mathfrak{D}^{nn'|q_1q_2q_3,\ell_1\ell_2\ell_3}_{q\mathbf{k}q'\mathbf{k}',\mathbf{p}} &= \delta(\Sigma^{qq'}_{n\mathbf{k}n'\mathbf{k}'} + q_1\Omega^{\ell_1,-q_1}_{\mathbf{p}} + q_2\Omega^{\ell_2,q_2}_{\mathbf{p}+q\mathbf{k}+q'\mathbf{k}'})\delta(\Delta^{qq'}_{n\mathbf{k}n'\mathbf{k}'} + 2q_3\Omega^{\ell_3,-q_3}_{\mathbf{p}+q'\mathbf{k}'} - q_1\Omega^{\ell_1,-q_1}_{\mathbf{p}} + q_2\Omega^{\ell_2,q_2}_{\mathbf{p}+\mathbf{q}\mathbf{k}+q'\mathbf{k}'}),\\ \mathfrak{F}^{q_1q_2q_4,\ell_1\ell_2\ell_3}_{q\mathbf{k}q'\mathbf{k}',\mathbf{p}} &= q_4(2n_{\mathrm{B}}(\Omega^{\ell_3,-q_3}_{\mathbf{p}+q'\mathbf{k}'}) + 1)(2n_{\mathrm{B}}(\Omega^{\ell_1,-q_1}_{\mathbf{p}}) + q_1 + 1)(2n_{\mathrm{B}}(\Omega^{\ell_2,q_2}_{\mathbf{p}+q\mathbf{k}+q'\mathbf{k}'}) + q_2 + 1).\end{aligned} \tag{20}$$

These formulas make no further assumptions on the nature of the spin-wave modes or spin-lattice couplings, so they could be applied to general problems involving spin-lattice couplings using a spin-wave approach. Note that although we take the spin-wave operators to be free bosons, with Gaussian correlations, the $Q^q_{n\mathbf{k}}$ operator defined through Eq. (15) is generally non-Gaussian, as it is bilinear in the b fields.

B. Square lattice two-sublattice antiferromagnets

Now, we evaluate the diagonal and Hall scattering rates specifically for spin waves on the square lattice in low magnetic fields. We assume the magnon dispersions $\Omega_{\ell,\mathbf{k}} = \sqrt{v_{\mathrm{m}}^2\underline{k}^2 + \Delta_\ell^2}$ ($\ell = 0, 1$ in this case), with magnon velocity v_{m} and magnon gaps Δ_ℓ, and take isotropic acoustic phonons with $\omega_{n\mathbf{k}} = v_{\mathrm{ph}}\sqrt{\underline{k}^2 + k_z^2}$ (we define $\underline{k} = \sqrt{k_x^2 + k_y^2}$). We obtain the coefficients $\mathcal{B}^{n\ell_1\ell_2|q_1q_2q}_{\mathbf{k};\mathbf{p}}$ from the continuum description of the spin waves in terms of local fluctuating uniform and staggered magnetization fields, and the symmetry-allowed couplings of these fields to the strain. The expressions for these coefficients are algebraically complicated, and some further details are given in Appendix B, with a full exposition of the calculations to be presented in a separate publication [32]. Here, instead, we sketch the important properties of the coefficients and their origins.

1. Scaling

First, when the temperature is smaller than the magnon gaps, $k_BT \lesssim \Delta_\ell$, all contributions to scattering become exponentially suppressed by thermal factors, and the scaling is unimportant. For larger temperatures, the gaps are negligible, and the momentum sum(s) in Eqs. (18) and (19) are dominated by momenta of order $k, p \sim k_BT/v_{\mathrm{m}}$. Then, the $\mathcal{B}$ coefficients, evaluated for momenta of this order, are sums of three types of contributions:

$$\mathcal{B} \sim \left(\frac{k_BT}{Mv_{\mathrm{ph}}^2}\right)^{\frac{1}{2}} n_0^{-1}\left(\lambda_{mm}\frac{\chi k_BT}{n_0} + \lambda_{mn} + \lambda_{nn}\frac{n_0}{\chi k_BT}\right). \tag{21}$$

Here, M is the mass per unit cell of the solid, n_0 is the ordered (staggered) moment density, χ is the uniform susceptibility, and $\lambda_{mm}, \lambda_{nn}$, and λ_{mn} represent couplings of the strain to exchange terms quadratic in local magnetization fluctuations δm, local staggered magnetization fluctuations δn, and the product of the two, respectively. Microscopically, this arises from effects like magnetostriction, the modification of orbital overlaps due to strain-induced bond length and angle changes, etc. The different powers of temperature multiplying the different λ couplings arise from the fact that the order parameter of the antiferromagnet is the staggered magnetization, and therefore, its fluctuations are more singular than those of the uniform magnetization, which is, however, still a low-energy mode in an antiferromagnet.

Depending upon the relative magnitudes of these different couplings, distinct scalings are observed for the diagonal and off-diagonal scattering rates, and hence for thermal conductivity components. To perform a full evaluation, we use parameters (given explicitly in Appendix B) that describe a typical situation corresponding to weak spin-orbit coupling and, correspondingly, weak anisotropy of magnetic exchange. In this case, there is a hierarchy that $\lambda_{mm} \gg \lambda_{nn}, \lambda_{mn}$ (which is ultimately a consequence of Goldstone's theorem). Furthermore, in the low-field regime, i.e., when the field-induced magnetization m_0 of the antiferromagnet is much smaller than m_s, the saturation value, $m_0 \ll m_s$, the mixed coupling λ_{mn} is proportional to m_0 and $\lambda_{mn} \ll \lambda_{nn}$ as well.

These facts allow one to estimate the scalings of the important physical quantities. The longitudinal scattering rate [Eq. (18)] scales as

$$D_{n\mathbf{k}} \sim \frac{1}{\tau} \sim T^{d-1}|\mathcal{B}|^2 \sim T^{d+2x}. \tag{22}$$

Here, d is the dimensionality of the spin system (which we later take equal to $d = 2$ for numerical calculations), while phonons are always three dimensional. The crucial exponent $x = 1$ occurs in the high-temperature regime dominated by λ_{mm}, while a crossover to behavior controlled by λ_{nn} with $x = -1$ can occur at lower temperatures if the minimum magnon gap is sufficiently small. This behavior corresponds to the longitudinal thermal conductivity [Eq. (8)] behaving as

$$\kappa_L \sim T^{3-d-2x}, \tag{23}$$

when magnon-phonon scattering dominates the phonon mean free path. Again, the power laws apply in certain distinct regimes and should be pieced together, along with the influence of nonzero gaps and other scattering mechanisms of phonons, to form a complete picture of the thermal conductivity. This is captured in the numerical calculations.

Next, we turn to the thermal Hall effect. It is crucial to keep in mind the *effective* time-reversal symmetry of an antiferromagnet under the combined action of time-reversal symmetry and a translation that exchanges the two sublattices. The uniform magnetization is invariant under this symmetry, but the staggered magnetization is odd. Consequently, the couplings λ_{mm} and λ_{nn} are even under effective time-reversal symmetry, while only λ_{mn} is odd. This implies that the Hall conductivity and Hall scattering rate $\mathfrak{W}^{\ominus,\mathrm{eff}}$, with $\mathfrak{W}^{\ominus,\mathrm{eff},qq'}_{n\mathbf{k},n'\mathbf{k}'} \coloneqq \mathfrak{W}^{\ominus,qq'}_{n\mathbf{k},n'\mathbf{k}'} + \mathfrak{W}^{\ominus,qq'}_{n-\mathbf{k},n'-\mathbf{k}'}$, which are odd under effective time-reversal symmetry, must be proportional to an odd power of λ_{mn}, and to linear order in the magnetic field or average magnetization, these quantities are simply linear in λ_{mn}. From Eqs. (19) and (21), we therefore obtain

$$\mathfrak{W}^{\ominus,\mathrm{eff}} \sim T^{d-1}\lambda_{mn}(\lambda_{mm}T + \lambda_{nn}T^{-1})^3 \sim T^{d-1+3x}. \quad (24)$$

The natural definition of a skew-scattering rate multiplies the above by a phase-space factor to account for the sum over different final states of the scattering, which gives $1/\tau_{\mathrm{skew}} \sim T^3\mathfrak{W}^{\ominus,\mathrm{eff}} \sim T^{d+2+3x}$.

We would like to emphasize that within any scattering mechanism of the phonon thermal Hall effect, the skew-scattering rate is a more fundamental measure of the chirality of the phonons than the thermal Hall *conductivity*. This is because the Hall conductivity inevitably involves the combination of the skew and longitudinal scattering rates (in the form $\tau^2/\tau_{\mathrm{skew}}$), and the longitudinal scattering rate of phonons has many other contributions that do not probe chirality and may have complex dependence on temperature and other parameters that obscure the skew scattering.

Consequently, instead of the thermal Hall conductivity, we discuss the thermal Hall resistivity ϱ_H, which is simply proportional to $1/\tau_{\mathrm{skew}}$, at least in the simplest view where the angle dependence of the longitudinal scattering does not spoil its cancellation.

We define the thermal Hall resistivity tensor as usual by the matrix inverse, $\boldsymbol{\varrho} = \boldsymbol{\kappa}^{-1}$. In particular, considering the simplest case of isotropic $\kappa^{\mu\mu} \to \kappa_L$ and $\kappa_L \gg \kappa^{\mu\neq\nu}$, one thus has

$$\varrho_H^{\mu\nu} = \frac{\varrho_{\mu\nu} - \varrho_{\nu\mu}}{2} \approx \frac{-\kappa_{\mu\nu} + \kappa_{\nu\mu}}{2\kappa_L^2} = -\frac{\kappa_H^{\mu\nu}}{\kappa_L^2}. \quad (25)$$

The quantity $\varrho_H^{\mu\nu}$ is independent of the scale of the longitudinal scattering, in the sense that under a rescaling $D_{n\mathbf{k}} \to \zeta D_{n\mathbf{k}}$, $\varrho_H^{\mu\nu}$ is unchanged. If we assume that $D_{n\mathbf{k}} = 1/\tau$ is $(n,\mathbf{k})$ independent, e.g., as is the case if dominated by some extrinsic effects, then we can readily extract the scaling of the thermal Hall resistivity. One finds

$$\varrho_H \sim \mathfrak{W}^{\ominus,\mathrm{eff}} \sim T^{d-1+3x}, \quad (26)$$

which is verified numerically. This scaling behavior should also be roughly true in the presence of more angle-dependent scattering, given the aforementioned independence on the scale of scattering.

Finally, we comment on the role of spin-orbit coupling in the present model. The coefficient λ_{mn} communicates the lack of effective time-reversal and mirror symmetry breaking to the scattering rate $\mathfrak{W}^{\ominus}$, and thereby, the Hall resistivity begins at linear order in this coefficient. In the present model, λ_{mn} is also proportional to (symmetric) spin-orbit coupling terms (microscopically, derivatives of such terms with respect to ionic displacement)—see Appendix B. In general, however, for more complex magnetic ordering patterns, a nonzero Hall effect may be obtained from our formulation even in the absence of spin-orbit coupling.

2. Numerical evaluation

It is important to verify that the formulas in Eqs. (18) and (19) are sufficient to generate all the expected symmetry-allowed scattering processes and thereby contributions to the thermal Hall conductivity. To do so, we evaluate these formulas numerically, which also allows a test of the scaling predictions above. In the numerical calculations, we take specific values for the microscopic parameters, which define the dispersions of the magnons and phonons, as well as those that underlie the $\mathcal{B}$ coefficients, comprising spin-lattice couplings and the mass per unit cell. Equations (8), (9), (18), and (19) were evaluated by a C code using the Cuba and Cubature libraries for numerical integration [34].

It is convenient to measure energies in units of the phononic energy scale $\epsilon_0 = k_B T_0 = \hbar v_{\mathrm{ph}}/\mathfrak{a}$, which is equal to the Debye temperature up to a factor, and we report thermal conductivities in units of $\kappa_0 = k_B v_{\mathrm{ph}}/\mathfrak{a}^2$, which gives a natural scale for phononic heat transport.

To make our numerical calculations more directly relevant, we choose key dimensionless parameters to loosely match those of Copper Deuteroformate Tetradeuterate (CFTD), a square lattice $S = 1/2$ antiferromagnet that has been intensively studied via neutron scattering [35–37] due to its convenient scale of exchange, which suits such measurements. For our purposes, CFTD has the desirable attribute that the magnon and phonon velocities are comparable (based on an estimate of the sound velocity from the corresponding hydrate [38]), which creates a significant phase space for magnon-phonon scattering. In particular, we take $v_{\mathrm{m}}/v_{\mathrm{ph}} = 2.5$, while the corresponding

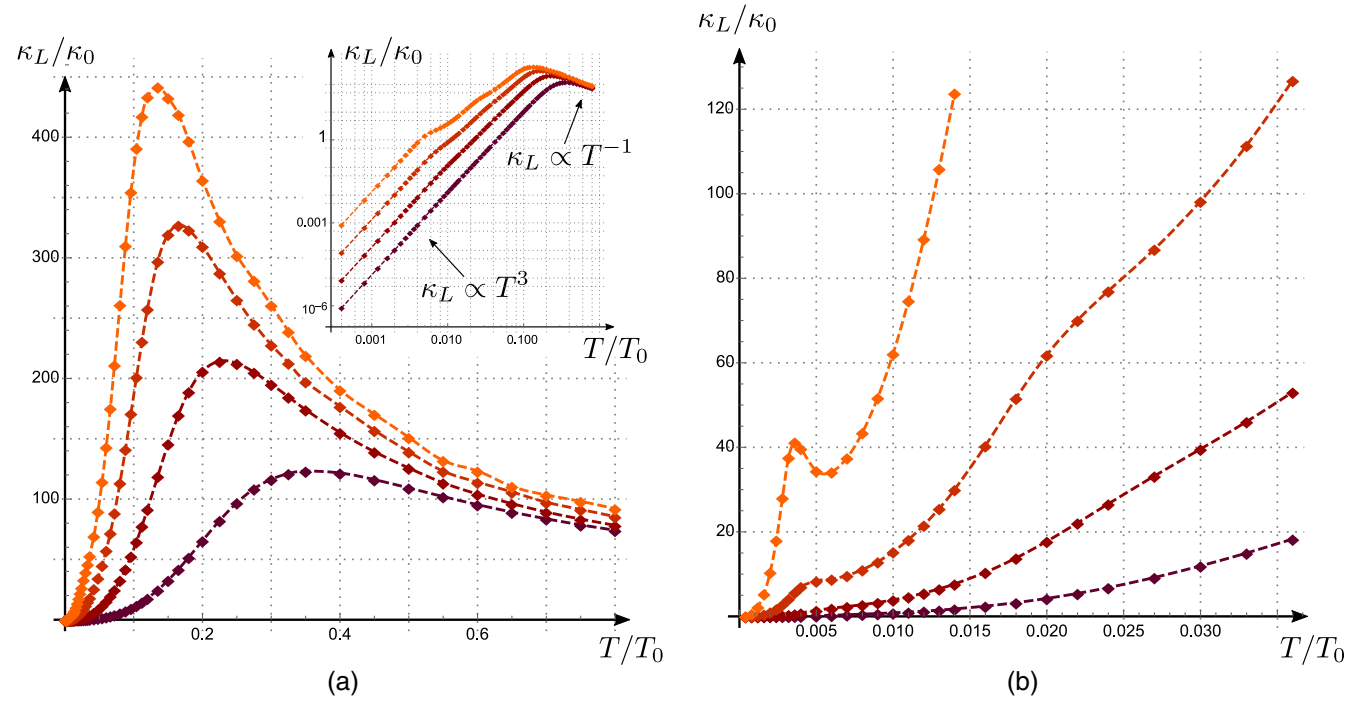

FIG. 3. Longitudinal thermal conductivity κ_L with respect to temperature T, for four different values of γ_{ext}. (a) Results on an order-one temperature scale, with $\gamma_{\text{ext}} = 1 \times 10^{-z}(v_{\text{ph}}/\mathfrak{a}), z \in [\![4, 7]\!]$, from darker ($z = 4$) to lighter ($z = 7$) shade. A crossover occurs between two scaling regimes with $x = 1$ and $x = -1$ [see Eq. (23)]. Inset: log-log plot. The scaling behaviors are consistent with the analysis presented in the text. (b) Results on a smaller temperature scale, with $\gamma_{\text{ext}} = 1 \times 10^{-z}(v_{\text{ph}}/\mathfrak{a}), z \in [\![6, 9]\!]$, from darker ($z = 6$) to lighter ($z = 9$) shade. The peaks are features related to the magnon gaps.

ratio in La_2CuO_4, $v_{\text{m}}/v_{\text{ph}}$, is approximately 30. We also use the mass per unit cell M_{uc} appropriate to CFTD. The parameters $n_0 = 1/2$ and $\chi = 1/(4J\mathfrak{a}^2)$ are chosen to be consistent with spin-wave theory. We include small magnon gaps, $\Delta_0 = 0.2\epsilon_0$ and $\Delta_1 = 0.04\epsilon_0$. The microscopic spin-lattice couplings are taken to be consistent with the expectations for weak spin-orbit coupling, and they are given in Appendix B. Finally, in the calculations, we include a small constant contribution $\check{D}_{n\mathbf{k}} \to \gamma_{\text{ext}}$, independent of $(n, \mathbf{k})$, to model additional scattering channels. In very clean monocrystals and in the absence of any other phonon scattering events, $\gamma_{\text{ext}} \sim v_{\text{ph}}/L$ reduces to the rate at which phonons bounce off the boundaries of the sample (of size L). We vary γ_{ext} to show the dependence on these extrinsic effects. For the calculations of the Hall effect, we include a small nonzero magnetization in the direction of the applied field, 1/20th of the saturation magnetization.

Figure 3 shows the results for the longitudinal thermal conductivity versus temperature in zero or low applied magnetic field (the results are insensitive to small magnetizations), for different choices of γ_{ext}. In panel (a), a broad temperature range is shown, which exposes the evolution from an extrinsic scattering regime $\kappa_L \propto T^3$ at low temperature to an intrinsic one $\kappa_L \propto 1/T$ at high temperature. In panel (b), further features emerge related to the scales of the magnon gaps.

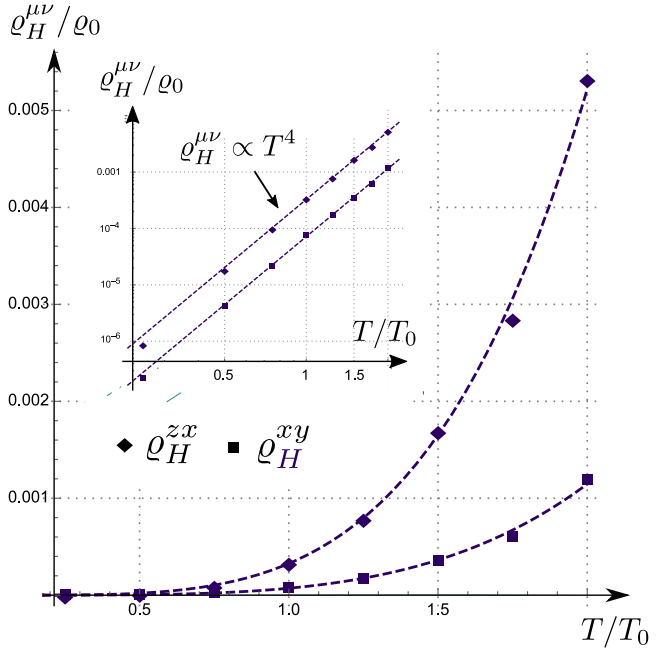

FIG. 4. Thermal Hall resistivity ϱ_H^{xy} and ϱ_H^{zx} (in units of $\varrho_0 = \kappa_0^{-1}$) with respect to temperature T. The transverse magnetization values (m_0^y, m_0^z) used for computing ϱ_H^{xy} and ϱ_H^{xz} are (0.0,0.05) and (0.05,0.0), respectively. Inset: log-log plot. The scaling behavior is consistent with the analysis presented in the text.

Next, we turn to the calculations of chiral scattering and the thermal Hall effect. Figure 2 shows a density plot of the Hall scattering rate $\mathfrak{W}^{\ominus,-+}$ as a function of the polar angle of $\mathbf{k}'$, $\theta(\mathbf{k}')$, and of the difference in azimuthal angles of $\mathbf{k}'$ and $\mathbf{k}$, $\varphi(\mathbf{k},\mathbf{k}') = \phi(\mathbf{k}') - \phi(\mathbf{k})$. We see that it has an intricate structure reflecting kinematics and energetics. The thermal Hall resistivity in the constant longitudinal scattering approximation ($D_{n\mathbf{k}} = 1/\tau$ independent of n, $\mathbf{k}$) is plotted in Fig. 4 for two different field orientations: For a field along the z axis, normal to the planes, we plot ϱ_H^{xy}, and for a field along the y axis, within the planes, we plot ϱ_H^{zx}. Both curves perfectly fit the T^4 scaling expected theoretically from Eq. (26) (using $d = 2, x = 1$) with weak spin-orbit coupling. Notably the magnitudes of the thermal Hall resistivity for the two orientations are comparable, and it is actually larger for an in-plane field than for an out-of-plane one.

IV. CONCLUSION

In this paper, we presented a theory for the skew scattering of phonons coupled to a quantum collective field, which gives rise to a phonon thermal Hall effect. A general formula, given in Eqs. (9) and (10), allows the latter to be calculated for *arbitrary* correlations of the collective variable. We then explicitly calculated these correlations for the case in which the collective field is bilinear in canonical bosons, e.g., spin-wave operators. A formula with no further assumptions is given in Eq. (19). Applying this to the regime of long-wavelength magnons in a square lattice antiferromagnet, we obtained a nonzero thermal Hall effect and its scaling with temperature in various regimes.

While we are not aware of any general results on the intrinsic phonon Hall conductivity due to scattering, there are a number of complementary theoretical papers, as well as some prior work, that overlap a small part of our results. The specific problem of phonons scattering from magnons was studied long ago to the leading second order in the coupling by Cottam [39]. That work, which assumed the isotropic SU(2) invariant limit, agrees with our calculations when these assumptions are imposed. The complementary mechanism of the intrinsic phonon Hall effect due to phonon Berry curvature was studied by many authors [23,40–42], including how the phonon Berry curvature is induced by spin-lattice coupling in Ref. [43]. The majority of recent theoretical work has concentrated on *extrinsic* effects due to scattering of phonons by defects [44–47]. The pioneering paper of Mori *et al.* [48], in particular, recognized the importance of higher-order contributions to scattering for the Hall effect and is in some ways a predecessor to our work.

Do the present results explain experiments on the cuprates? We have not attempted a quantitative comparison, for several reasons. This would require some detailed knowledge of spin-lattice couplings. It also is numerically difficult because in the cuprates there is a very large ratio of magnon to phonon velocities (of order 30), which renders the scattering phase space narrow and the integration challenging. Nevertheless, it is interesting to ask about the order of magnitude of the response. For this comparison, we follow the logic outlined in Sec. III B 1 in which we argued that the thermal Hall resistivity is a better quantity for which to compare theory and experiment. We obtain the thermal resistivity from the experimental data in Ref. [18] on the undoped material La_2CuO_4: At about 20 K, the longitudinal conductivity $\kappa_{xx} \approx 10$ W/(K m) (from their extended data in Fig. 2), and the thermal Hall conductivity $\kappa_{xy} \approx 40$ mW/(K m). Using Eq. (25) and the value $\varrho_0^{\mathrm{LCO}} \approx 2.6$ K m/W, we then obtain $(\varrho_H/\varrho_0)^{\mathrm{LCO}} \approx 1.5 \times 10^{-4}$. This is at least comparable to values in Fig. 4.

Regardless of whether the intrinsic picture is correct for the cuprates (we think it is most promising for systems like CFTD for which there is a good phase-space match of phonons and magnons), we believe that a scattering mechanism of some kind is very likely at work. Therefore, we would encourage the analysis of future experimental data in terms of ϱ_H rather than κ_H.

In a companion paper [32], we will expound on the results of the present paper and give several extensions covering even more general types of coupling of phonons to collective degrees of freedom. There also remain many other related problems that would be interesting to explore, for example, the influence of electronic disequilibrium upon the phonons, and vice versa, and the interplay of scattering, presumed here to be dominant, and phononic Berry phases. We hope that the present study provides a theoretical framework to begin to approach these and other intriguing questions.

ACKNOWLEDGMENTS

We thank Mengxing Ye for valuable discussions, as well as Xiao Chen and Jason Iaconis for a collaboration on a related topic. We also sincerely acknowledge Roser Valentí for her encouragement and enthusiasm. The premises of this project were funded by the Agence Nationale de la Recherche through Grant No. ANR-18-ERC2-0003-01 (QUANTEM). The bulk of this project was funded by the European Research Council (ERC) under the European Union's Horizon 2020 research and innovation program (Grant Agreement No. 853116, acronym TRANSPORT). L. B. was supported by the U.S. Department of Energy, Office of Science, Basic Energy Sciences under Award No. DE-FG02-08ER46524. It befits us to acknowledge the hospitality of the KITP, where part of this project was carried out, funded under the National Science Foundation Grant No. NSF PHY-1748958.

APPENDIX A: FROM INTERACTION TERMS TO THE COLLISION INTEGRAL

1. First Born order

First, we consider only the first term of Born's expansion. The transition rate associated with H' at this order derives from the matrix elements:

$$T^{[1]}_{\mathtt{i}\to\mathtt{f}} = \sum_{n\mathbf{k}q} \sqrt{N^i_{\mathbf{k},n} + \frac{q+1}{2}} \langle f_s | Q^q_{n\mathbf{k}} | i_s \rangle \mathbb{I}(i_p \overset{q\cdot n\mathbf{k}}{\to} f_p), \quad \text{(A1)}$$

where $\mathbb{I}(i_p \overset{q\cdot n\mathbf{k}}{\to} f_p)$ means that the only difference between $|i_p\rangle$ and $|f_p\rangle$ is that there is $q = \pm 1$ more phonon of species $(n, \mathbf{k})$ in the final state.

We then compute the squared matrix element. We have

$$|T^{[1]}_{\mathtt{i}\to\mathtt{f}}|^2 = \sum_{n\mathbf{k}q} \left(N^i_{\mathbf{k},n} + \frac{q+1}{2} \right) \mathbb{I}(i_p \overset{q\cdot n\mathbf{k}}{\to} f_p) \times \langle i_s | Q^{-q}_{n\mathbf{k}} | f_s \rangle \langle f_s | Q^q_{n\mathbf{k}} | i_s \rangle. \quad \text{(A2)}$$

Next, we enforce the energy conservation $\delta(E_\mathtt{f} - E_\mathtt{i}) = \delta(q\omega_{n\mathbf{k}} + E_{f_s} - E_{i_s})$ by writing the latter as a time integral, i.e., $\int_{-\infty}^{+\infty} \mathrm{d}t e^{i\omega t} = 2\pi\delta(\omega)$; identify $A(t) = e^{+iHt} A e^{-iHt}$; use the identity $1 = \sum_{f_s} |f_s\rangle\langle f_s|$; and take the Q field in the initial state to be in thermal equilibrium, $p_{i_s} = Z_s^{-1} e^{-\beta E_{i_s}}$. Finally summing over $|i_s\rangle$ and identifying $\langle A \rangle_\beta = Z_s^{-1} \mathrm{Tr}(e^{-\beta H} A)$, we find that the scattering rate between phonon states at first Born order reads

$$\Gamma^{[1];[1]}_{i_p\to f_p} = \sum_{n\mathbf{k}q} \left(N^i_{n\mathbf{k}} + \frac{q+1}{2} \right) \mathbb{I}(i_p \overset{q\cdot n\mathbf{k}}{\to} f_p) \times \int_{-\infty}^{\infty} dt e^{-iq\omega_{n\mathbf{k}}t} \langle Q^{-q}_{n\mathbf{k}}(t) Q^q_{n\mathbf{k}}(0) \rangle_\beta. \quad \text{(A3)}$$

To arrive at the collision integral, the final step involves summing over final phononic states f_p and taking the average over initial phononic states i_p. First, we notice that a change of variables in $\langle Q^{-q}_{n\mathbf{k}}(t) Q^q_{n\mathbf{k}}(0) \rangle_\beta$ leads to the detailed-balance relation

$$\langle Q^{-q}_{n\mathbf{k}}(t) Q^q_{n\mathbf{k}}(0) \rangle_\beta = \langle Q^q_{n\mathbf{k}}(t) Q^{-q}_{n\mathbf{k}}(0) \rangle_\beta e^{-q\beta\omega_{n\mathbf{k}}}. \quad \text{(A4)}$$

It is then straightforward to show that only the commutator term on the right-hand side of Eq. (A3) satisfies this relation. In turn, the final expression for the diagonal of the collision matrix takes the form of the spectral function:

$$D^{[1];[1]}_{n\mathbf{k}} = -\int_{-\infty}^{+\infty} dt e^{-i\omega_{n\mathbf{k}}t} \langle [Q^-_{n\mathbf{k}}(t), Q^+_{n\mathbf{k}}(0)] \rangle_\beta, \quad \text{(A5)}$$

as quoted in the main text.

2. Second Born order

As discussed, the first Born approximation alone does not lead to a nonzero thermal Hall effect. Here, we compute what appears when the Born expansion is taken up to the second Born order. We have

$$T^{[1,1]}_{\mathtt{i}\to\mathtt{f}} = \sum_{n\mathbf{k},n'\mathbf{k}'} \sum_{q,q'=\pm} \sqrt{N^i_{n\mathbf{k}} + \frac{1+q}{2}} \sqrt{N^f_{n'\mathbf{k}'} + \frac{1-q'}{2}} \times \sum_{m_s} \frac{\langle f_s | Q^{q'}_{n'\mathbf{k}'} | m_s \rangle \langle m_s | Q^q_{n\mathbf{k}} | i_s \rangle}{E_{i_s} - E_{m_s} - q\omega_{\mathbf{k},n} + i\eta} \mathbb{I}(i_p \overset{q\cdot n\mathbf{k}}{\underset{q'\cdot n'\mathbf{k}'}{\to}} f_p). \quad \text{(A6)}$$

The squared T-matrix elements now include cross terms between the first and second orders of the Born expansion. Here, we give details of the calculation of one term, the square of Eq. (A6), $|T^{[1,1]}_{\mathtt{i}\to\mathtt{f}}|^2$. In the numerator, the matrix elements of the Q operators can combine in two different ways, which we denote in the following as (a) $\langle i_s | Q^q_{n\mathbf{k}} | m_s \rangle \langle m_s | Q^{q'}_{n'\mathbf{k}'} | f_s \rangle \langle f_s | Q^{-q'}_{n'\mathbf{k}'} | m'_s \rangle \langle m'_s | Q^{-q}_{n\mathbf{k}} | i_s \rangle$ and (b) $\langle i_s | Q^q_{n\mathbf{k}} | m_s \rangle \langle m_s | Q^{q'}_{n'\mathbf{k}'} | f_s \rangle \langle f_s | Q^{-q}_{n\mathbf{k}} | m'_s \rangle \langle m'_s | Q^{-q'}_{n'\mathbf{k}'} | i_s \rangle$.

We use the following time integral representation of each of the denominators (using a regularized definition of the sign function),

$$\frac{1}{x \pm i\eta} = PP\frac{1}{x} \mp i\pi\delta(x) = \frac{1}{2i}\int_{-\infty}^{+\infty} dt_1 e^{it_1 x} \mathrm{sign}(t_1) \pm \frac{1}{2i}\int_{-\infty}^{+\infty} dt_1 e^{it_1 x} \quad \text{(A7)}$$

and introduce a third time integral to enforce the energy conservation $E_\mathtt{f} - E_\mathtt{i} = q'\omega_{n'\mathbf{k}'} + q\omega_{n\mathbf{k}} + E_{f_s} - E_{i_s}$. The product of the denominators [cf. Eq. (A7)] leads to four terms, which can be labeled by two signs $s, s' = \pm$, and we define, for convenience,

$$\Theta_{ss'}(t_1, t_2) \coloneqq [-\mathrm{sign}(t_1)]^{\frac{1-s}{2}} [\mathrm{sign}(t_2)]^{\frac{1-s'}{2}}. \quad \text{(A8)}$$

Then, the transition rate coming from this part of the total squared matrix element can be written as a sum of eight terms:

$$\Gamma^{[1,1];[1,1]}_{i_p\to f_p} = \sum_{n\mathbf{k},n'\mathbf{k}'} \sum_{q,q'} \left(N^i_{n\mathbf{k}} + \frac{q+1}{2} \right) \left(N^i_{n'\mathbf{k}'} + \frac{q'+1}{2} \right) \times \sum_{s,s'=\pm} \sum_{i=a,b} W^{[1,1];[1,1],(i),ss'}_{n\mathbf{k}q,n'\mathbf{k}'q'} \mathbb{I}(i_p \overset{q\cdot n\mathbf{k}}{\underset{q'\cdot n'\mathbf{k}'}{\to}} f_p), \quad \text{(A9)}$$

where we defined (notice the order of the first two operators in the correlator and the sign $t_1 \pm t_2$ in the exponential):

$$W^{[1,1];[1,1],(a),ss'}_{n\mathbf{k}q,n'\mathbf{k}'q'} = \int dt dt_1 dt_2 \Theta_{ss'}(t_1, t_2) e^{i(q\omega_{n\mathbf{k}} + q'\omega_{n'\mathbf{k}'})t} e^{i(t_1+t_2)(q\omega_{n\mathbf{k}} - q'\omega_{n'\mathbf{k}'})} \times \langle Q^{-q}_{n\mathbf{k}}(-t-t_2) Q^{-q'}_{n'\mathbf{k}'}(-t+t_2) Q^{q'}_{n'\mathbf{k}'}(-t_1) Q^q_{n\mathbf{k}}(+t_1) \rangle_\beta, \quad \text{(A10)}$$

$$W^{[1,1];[1,1],(b),ss'}_{n\mathbf{k}q,n'\mathbf{k}'q'} = \int dt dt_1 dt_2 \Theta_{ss'}(t_1,t_2) e^{i(q\omega_{n\mathbf{k}}+q'\omega_{n'\mathbf{k}'})t} e^{i(t_1-t_2)(q\omega_{n\mathbf{k}}-q'\omega_{n'\mathbf{k}'})} \times \langle Q^{-q'}_{n'\mathbf{k}'}(-t-t_2) Q^{-q}_{n\mathbf{k}}(-t+t_2) Q^{q'}_{n'\mathbf{k}'}(-t_1) Q^{q}_{n\mathbf{k}}(+t_1)\rangle_\beta. \quad \text{(A11)}$$

One can show the following ("anti-")detailed-balance relations:

$$W^{[1,1];[1,1],(a),ss'}_{n\mathbf{k}q,n'\mathbf{k}'q'} = ss' W^{[1,1];[1,1],(a),s's}_{n'\mathbf{k}'-q',n\mathbf{k}-q} e^{-\beta(q\omega_{n\mathbf{k}}+q'\omega_{n'\mathbf{k}'})}, \quad \text{(A12)}$$

$$W^{[1,1];[1,1],(b),ss'}_{n\mathbf{k}q,n'\mathbf{k}'q'} = ss' W^{[1,1];[1,1],(b),s's}_{n\mathbf{k}-q,n'\mathbf{k}'-q'} e^{-\beta(q\omega_{n\mathbf{k}}+q'\omega_{n'\mathbf{k}'})}. \quad \text{(A13)}$$

From this, the same holds for the symmetrized in $n\mathbf{k}q \leftrightarrow n'\mathbf{k}'q'$ scattering rate $\mathcal{W}^{[1,1];[1,1],ss'}_{n\mathbf{k}q,n'\mathbf{k}'q'} = \sum_{i=a,b} W^{[1,1];[1,1],(i),ss'}_{n\mathbf{k}q,n'\mathbf{k}'q'} + (n\mathbf{k}q \leftrightarrow n'\mathbf{k}'q')$, i.e.,

$$\mathcal{W}^{[1,1];[1,1],ss'}_{n\mathbf{k}q,n'\mathbf{k}'q'} = ss' e^{-\beta(q\omega_{n\mathbf{k}}+q'\omega_{n'\mathbf{k}'})} \mathcal{W}^{[1,1];[1,1],ss'}_{n\mathbf{k}-q,n'\mathbf{k}'-q'}. \quad \text{(A14)}$$

We can then identify

$$\mathfrak{W}^{\ominus,[1,1];[1,1],qq'}_{n\mathbf{k},n'\mathbf{k}'} = N_{\mathrm{uc}} \sum_{s=\pm} \mathcal{W}^{[1,1];[1,1],s,-s}_{n\mathbf{k}q,n'\mathbf{k}'q'}, \quad \text{(A15)}$$

$$\mathfrak{W}^{\oplus,[1,1];[1,1],qq'}_{n\mathbf{k},n'\mathbf{k}'} = N_{\mathrm{uc}} \sum_{s=\pm} \mathcal{W}^{[1,1];[1,1],ss}_{n\mathbf{k}q,n'\mathbf{k}'q'}, \quad \text{(A16)}$$

which, by construction, satisfy

$$\mathfrak{W}^{\sigma,[1,1];[1,1],qq'}_{n\mathbf{k},n'\mathbf{k}'} = \sigma e^{-\beta(q\omega_{n\mathbf{k}}+q'\omega_{n'\mathbf{k}'})} \mathfrak{W}^{\sigma,[1,1];[1,1],-q-q'}_{n\mathbf{k},n'\mathbf{k}'}, \quad \text{(A17)}$$

where $\sigma = \oplus$ (respectively, $\sigma = \ominus$) indicates that $\mathfrak{W}$ satisfies detailed balance (respectively, anti-detailed balance). Only $\mathfrak{W}^{\ominus,[1,1];[1,1],qq'}_{n\mathbf{k},n'\mathbf{k}'}$ contributes to the thermal Hall conductivity.

APPENDIX B: DETAILS OF THE MAGNETIC MODEL

1. General symmetry-allowed model

We begin with a semimicroscopic coupling of the local strain tensor $\boldsymbol{\mathcal{E}}_{\mathbf{r}}$ to continuum nonlinear sigma-model fields: the density m_a of uniform magnetization and n_a of staggered magnetization ($a = x, y, z$), which is

$$\mathcal{H}'_{\mathrm{tetra}}(\mathbf{r}) = \sum_{\substack{\alpha,\beta=x,y,z \\ a,b=x,y,z}} \mathcal{E}^{\alpha\beta}_{\mathbf{r}} \left(\Lambda^{(\mathrm{n}),\alpha\beta}_{ab} \mathrm{n}_a \mathrm{n}_b + \frac{\Lambda^{(\mathrm{m}),\alpha\beta}_{ab}}{n_0^2} \mathrm{m}_a \mathrm{m}_b \right)\Big|_{\mathbf{x},z}, \quad \text{(B1)}$$

where n_0 is the ordered moment density. The $\Lambda^{(\xi),\alpha\beta}_{ab}$ coefficients are constrained by the tetragonal symmetry of the crystal. The nonlinear sigma model is defined by the constraints $\mathbf{n}\cdot\mathbf{m} = 0$ and $\mathbf{n}^2 + \mathbf{m}^2/n_0^2 = 1$.

We expand the above to second order in the fluctuations $(\delta m, \delta n)$ around the average values due to both spontaneous ordering and the applied field. We take the Néel vector along $\hat{\boldsymbol{x}}$. Then, $\mathrm{n}_x = 1 - \frac{1}{2}\sum_{b=y,z}[\delta n_b^2 + (1/n_0^2)(m_0^b + \delta m_b)^2]$, and $\mathrm{m}_x = -\sum_{b=y,z}(m_0^b + \delta m_b)\delta n_b$. Here, $\boldsymbol{m}_0$ is the average uniform magnetization, which lies in the $y-z$ plane. We assume $m_0 \ll n_0$, so quantities are expressed to linear order in m_0 whenever possible. This gives

$$\mathcal{H}'_{\mathrm{tetra}}(\mathbf{r}) \approx \sum_{\alpha\beta} \mathcal{E}^{\alpha\beta}_{\mathbf{r}} \sum_{a,b=y,z} \sum_{\xi,\xi'=0,1} \lambda^{\alpha\beta}_{ab;\xi\xi'} n_0^{-\xi-\xi'} \eta_{a\xi\mathbf{r}} \eta_{b\xi'\mathbf{r}}, \quad \text{(B2)}$$

where $\eta_{a0} = \delta n_a$ and $\eta_{a1} = \delta m_a$, and

$$\lambda^{\alpha\beta}_{ab;\xi\xi} = \Lambda^{(\xi),\alpha\beta}_{ab} - \delta_{ab}\Lambda^{(0),\alpha\beta}_{xx},$$
$$\lambda^{\alpha\beta}_{ab;01} = \lambda^{\alpha\beta}_{ba;10} = \frac{-1}{n_0}[m_0^a \Lambda^{(1),\alpha\beta}_{bx} + \delta_{ab} m_0^{\bar{a}} \Lambda^{(1),\alpha\beta}_{\bar{a}x} + m_0^b \Lambda^{(0),\alpha\beta}_{ax}], \quad \text{(B3)}$$

where $\bar{y} = z$, $\bar{z} = y$ and we have associated $\xi = \mathrm{n} \Leftrightarrow \xi = 0$ and $\xi = \mathrm{m} \Leftrightarrow \xi = 1$ in $\Lambda^{(\xi)}$.

Here, each $\Lambda^{(\xi)}$ tensor, which we define to be symmetric in both ab and $\alpha\beta$ variables, has seven independent coefficients, which we call $\Lambda^{(\xi)}_1 = \Lambda^{(\xi),xx}_{xx} = \Lambda^{(\xi),yy}_{yy}$, $\Lambda^{(\xi)}_2 = \Lambda^{(\xi),xx}_{yy} = \Lambda^{(\xi),yy}_{xx}$, $\Lambda^{(\xi)}_3 = \Lambda^{(\xi),xx}_{zz} = \Lambda^{(\xi),yy}_{zz}$, $\Lambda^{(\xi)}_4 = \Lambda^{(\xi),zz}_{xx} = \Lambda^{(\xi),zz}_{yy}$, $\Lambda^{(\xi)}_5 = \Lambda^{(\xi),zz}_{zz}$, $\Lambda^{(\xi)}_6 = \Lambda^{(\xi),xy}_{xy} = \Lambda^{(\xi),yx}_{xy} = \Lambda^{(\xi),yx}_{yx} = \Lambda^{(\xi),xy}_{yx}$, and $\Lambda^{(\xi)}_7 = \Lambda^{(\xi),xz}_{xz} = \Lambda^{(\xi),zx}_{xz} = \Lambda^{(\xi),zx}_{zx} = \Lambda^{(\xi),xz}_{zx} = \Lambda^{(\xi),yz}_{yz} = \Lambda^{(\xi),zy}_{yz} = \Lambda^{(\xi),zy}_{zy} = \Lambda^{(\xi),yz}_{zy}$. All other $\Lambda^{(\xi),\alpha\beta}_{ab}$ are zero. This is the most general coupling allowed by the symmetries of the lattice and of magnetic order.

To cast this in the form of Eqs. (2) and (15), we insert the (very standard) free field expressions for the strain and magnetization fluctuations in terms of phonon and magnon creation or annihilation operators, respectively, into Eq. (B2). For the strain,

$$\mathcal{E}^{\mu\nu}(\mathbf{x}) = \frac{1}{\sqrt{V}} \sum_{n\mathbf{k}} \frac{i/2}{\sqrt{2\rho_M \omega_{n\mathbf{k}}}} (a_{n\mathbf{k}} + a^\dagger_{n,-\mathbf{k}})(k^\mu \varepsilon^\nu_{n\mathbf{k}} + k^\nu \varepsilon^\mu_{n\mathbf{k}}) e^{i\mathbf{k}\cdot\mathbf{x}}, \quad \text{(B4)}$$

where ρ_M is the mass density. For the magnetization densities, diagonalization of the nonlinear sigma-model Hamiltonian density

TABLE I. Numerical values of the fixed dimensionless parameters used in all numerical evaluations. The upper and lower entries for m_0^y and m_0^z correspond to the two cases for calculating ϱ_H^{xy} and ϱ_H^{xz}, respectively. The couplings $\Lambda_i^{(\xi)}$ are given in units of $\epsilon_0/\mathfrak{a}$.

$\frac{v_{\mathrm{m}}}{v_{\mathrm{ph}}}$	$\chi\epsilon_0\mathfrak{a}^2$	n_0	$\frac{M_{\mathrm{uc}}v_{\mathrm{ph}}\mathfrak{a}}{\hbar}$	m_0^x	m_0^y	m_0^z	$\frac{\Delta_0}{\epsilon_0}$	$\frac{\Delta_1}{\epsilon_0}$
					0.0	0.05		
2.5	0.19	1/2	8×10^3	0			0.2	0.04
					0.05	0.0		

ξ	$\Lambda_1^{(\xi)}$	$\Lambda_2^{(\xi)}$	$\Lambda_3^{(\xi)}$	$\Lambda_4^{(\xi)}$	$\Lambda_5^{(\xi)}$	$\Lambda_6^{(\xi)}$	$\Lambda_7^{(\xi)}$
$n=0$	12.0	10.0	14.0	10.0	12.0	0.6	0.8
$m=1$	−10.0	−12.0	−14.0	−12.0	−10.0	−0.8	−0.6

$$\mathcal{H}_m = \frac{\rho}{2}(|\underline{\nabla}\delta n_y|^2 + |\underline{\nabla}\delta n_z|^2) + \frac{1}{2\chi}(\delta m_y^2 + \delta m_z^2) + \sum_{a=y,z}\frac{\chi\Delta_{a-1}^2}{2}\delta n_a^2 \quad \text{(B5)}$$

yields

$$\eta_{a\xi\mathbf{r}} = \sum_{\mathbf{p}}\sum_{\ell=0,1}\sum_{q=\pm} U_{a\xi\ell q}(\mathbf{p}) b_{\ell\mathbf{p}}^q e^{i\mathbf{p}\cdot\mathbf{r}}, \quad \text{(B6)}$$

with

$$U_{a\xi\ell q}(\mathbf{p}) = -\delta_{a-1,\ell-\bar{\xi} \bmod 2} F_{\xi q\ell}(\mathbf{p}), \quad \text{(B7)}$$

$$F_{\xi q\ell}(\mathbf{p}) = (iq)^{\bar{\xi}}(-1)^{\bar{\xi}\ell}(\chi\Omega_{\ell\mathbf{p}})^{\xi-\frac{1}{2}}. \quad \text{(B8)}$$

We defined $\bar{\xi} = 1-\xi$, i.e., $\bar{0}=1, \bar{1}=0$, as well as $a = y \Leftrightarrow a-1=0$ and $a=z \Leftrightarrow a-1=1$. In addition, in Eq. (B5), ρ is the antiferromagnetic spin stiffness, and χ is the magnetic susceptibility. Inserting these definitions into Eq. (B2), some algebra leads to the form given in Eqs. (14) and (15), with the coupling coefficients

$$\mathcal{B}_{\mathbf{k};\mathbf{p}}^{n,\ell_1\ell_2|q_1q_2q} = \frac{iq}{2\sqrt{2M_{\mathrm{uc}}}}\sum_{\xi\xi'} n_0^{-\xi-\xi'}\mathcal{L}_{n\mathbf{k};\xi,\xi'}^{q,\ell_1,\ell_2} F_{\xi q_1\ell_1}\left(\mathbf{p}+\frac{q}{2}\mathbf{k}\right) \times F_{\xi' q_2\ell_2}\left(-\mathbf{p}+\frac{q}{2}\mathbf{k}\right), \quad \text{(B9)}$$

where

$$\mathcal{L}_{n\mathbf{k};\xi,\xi'}^{q,\ell_1,\ell_2} = \sum_{\alpha,\beta=x,y,z}\hat{\lambda}_{\xi\xi'}^{\ell_1\ell_2;\alpha\beta}\frac{k^\alpha(\varepsilon_{n\mathbf{k}}^\beta)^q + k^\beta(\varepsilon_{n\mathbf{k}}^\alpha)^q}{\sqrt{\omega_{n\mathbf{k}}}}, \quad \text{(B10)}$$

and $\hat{\lambda}_{\xi\xi'}^{\ell\ell';\alpha\beta} = \lambda_{\ell-\bar{\xi}\mathrm{mod}2,\ell'-\bar{\xi}'\mathrm{mod}2;\xi\xi'}^{\alpha\beta}$.

Note that the λ_{mn} coefficients involved in the Hall conductivity, namely, the $\boldsymbol{\lambda}_{ab;01}$ rank-2 tensors, are written explicitly in Eq. (B3). They are proportional to the net magnetization $\boldsymbol{m}_0$, as is consistent with the fact that they are associated with a time-reversal breaking quantity. One can also observe that they involve only the *anisotropic* coefficients $\Lambda_{6,7}^{(\xi)}$, which, in a microscopic derivation, arise from spin-orbit coupling; see Ref. [32].

2. Numerical implementation

In the numerical implementation, we use values of the parameters roughly appropriate for CFTD, which we provide in Table I. The phonon polarization vectors $\boldsymbol{\varepsilon}_{n,\mathbf{k}}$ are chosen to form an orthonormal basis in which $\mathbf{k}$ points along the $[1,1,1]$ axis, so $\mathbf{k}\cdot\boldsymbol{\varepsilon}_{n,\mathbf{k}} = (|\mathbf{k}|/\sqrt{3})\ \forall\, n$.

[1] Minoru Yamashita, Norihito Nakata, Yoshinori Senshu, Masaki Nagata, Hiroshi M. Yamamoto, Reizo Kato, Takasada Shibauchi, and Yuji Matsuda, *Highly Mobile Gapless Excitations in a Two-Dimensional Candidate Quantum Spin Liquid*, Science **328**, 1246 (2010).

[2] Y. Kasahara, T. Ohnishi, Y. Mizukami, O. Tanaka, Sixiao Ma, K. Sugii, N. Kurita, H. Tanaka, J. Nasu, Y. Motome, T. Shibauchi, and Y. Matsuda, *Majorana Quantization and Half-Integer Thermal Quantum Hall Effect in a Kitaev Spin Liquid*, Nature (London) **559**, 227 (2018).

[3] Gaël Grissonnanche, Anaëlle Legros, Sven Badoux, Etienne Lefrançois, Victor Zatko, Maude Lizaire, Francis Laliberté, Adrien Gourgout, J-S Zhou, Sunseng Pyon *et al.*, *Giant Thermal Hall Conductivity in the Pseudogap Phase of Cuprate Superconductors*, Nature (London) **571**, 376 (2019).

[4] Marie-Eve Boulanger, Gaël Grissonnanche, Sven Badoux, Andréanne Allaire, Étienne Lefrançois, Anaëlle Legros, Adrien Gourgout, Maxime Dion, CH Wang, XH Chen *et al.*, *Thermal Hall Conductivity in the Cuprate Mott Insulators* Nd_2CuO_4 *and* $Sr_2CuO_2Cl_2$, Nat. Commun. **11**, 5325 (2020).

[5] H. B. G. Casimir, *On Onsager's Principle of Microscopic Reversibility*, Rev. Mod. Phys. **17**, 343 (1945).

[6] Hosho Katsura, Naoto Nagaosa, and Patrick A. Lee, *Theory of the Thermal Hall Effect in Quantum Magnets*, Phys. Rev. Lett. **104**, 066403 (2010).

[7] Jung Hoon Han and Hyunyong Lee, *Spin Chirality and Hall-Like Transport Phenomena of Spin Excitations*, J. Phys. Soc. Jpn. **86**, 011007 (2017).

[8] Jung Hoon Han, Jin-Hong Park, and Patrick A. Lee, *Consideration of Thermal Hall Effect in Undoped Cuprates*, Phys. Rev. B **99**, 205157 (2019).

[9] Rhine Samajdar, Shubhayu Chatterjee, Subir Sachdev, and Mathias S. Scheurer, *Thermal Hall Effect in Square-Lattice Spin Liquids: A Schwinger Boson Mean-Field Study*, Phys. Rev. B **99**, 165126 (2019).

[10] Yanting Teng, Yunchao Zhang, Rhine Samajdar, Mathias S. Scheurer, and Subir Sachdev, *Unquantized Thermal Hall Effect in Quantum Spin Liquids with Spinon Fermi Surfaces*, Phys. Rev. Res. **2**, 033283 (2020).

[11] Ryo Matsumoto and Shuichi Murakami, *Rotational Motion of Magnons and the Thermal Hall Effect*, Phys. Rev. B **84**, 184406 (2011).
[12] Shuichi Murakami and Akihiro Okamoto, *Thermal Hall Effect of Magnons*, J. Phys. Soc. Jpn. **86**, 011010 (2017).
[13] Alexander Mook, Jürgen Henk, and Ingrid Mertig, *Thermal Hall Effect in Noncollinear Coplanar Insulating Antiferromagnets*, Phys. Rev. B **99**, 014427 (2019).
[14] Shinnosuke Koyama and Joji Nasu, *Field-Angle Dependence of Thermal Hall Conductivity in a Magnetically Ordered Kitaev-Heisenberg System*, Phys. Rev. B **104**, 075121 (2021).
[15] Yuji Hirokane, Yoichi Nii, Yasuhide Tomioka, and Yoshinori Onose, *Phononic Thermal Hall Effect in Diluted Terbium Oxides*, Phys. Rev. B **99**, 134419 (2019).
[16] Xiaokang Li, Benoît Fauqué, Zengwei Zhu, and Kamran Behnia, *Phonon Thermal Hall Effect in Strontium Titanate*, Phys. Rev. Lett. **124**, 105901 (2020).
[17] Lu Chen, Marie-Eve Boulanger, Zhi-Cheng Wang, Fazel Tafti, and Louis Taillefer, *Large Phonon Thermal Hall Conductivity in a Simple Antiferromagnetic Insulator*, Proc. Natl. Acad. Sci. U.S.A. **119**, e2208016119 (2022).
[18] G. Grissonnanche, S. Thériault, A. Gourgout, M.-E. Boulanger, E. Lefrançois, A. Ataei, F. Laliberté, M. Dion, J.-S. Zhou, S. Pyon *et al.*, *Chiral Phonons in the Pseudogap Phase of Cuprates*, Nat. Phys. **16**, 1108 (2020).
[19] L. Sheng, D. N. Sheng, and C. S. Ting, *Theory of the Phonon Hall Effect in Paramagnetic Dielectrics*, Phys. Rev. Lett. **96**, 155901 (2006).
[20] Yu. Kagan and L. A. Maksimov, *Anomalous Hall Effect for the Phonon Heat Conductivity in Paramagnetic Dielectrics*, Phys. Rev. Lett. **100**, 145902 (2008).
[21] Xiaoou Zhang, Yinhan Zhang, Satoshi Okamoto, and Di Xiao, *Thermal Hall Effect Induced by Magnon-Phonon Interactions*, Phys. Rev. Lett. **123**, 167202 (2019).
[22] Jing-Yuan Chen, Steven A. Kivelson, and Xiao-Qi Sun, *Enhanced Thermal Hall Effect in Nearly Ferroelectric Insulators*, Phys. Rev. Lett. **124**, 167601 (2020).
[23] Takuma Saito, Kou Misaki, Hiroaki Ishizuka, and Naoto Nagaosa, *Berry Phase of Phonons and Thermal Hall Effect in Nonmagnetic Insulators*, Phys. Rev. Lett. **123**, 255901 (2019).
[24] T. Holstein, *Studies of Polaron Motion: Part I. The Molecular-Crystal Model*, Ann. Phys. (N.Y.) **8**, 325 (1959).
[25] T. Holstein, *Studies of Polaron Motion: Part II. The "Small" Polaron*, Ann. Phys. (N.Y.) **8**, 343 (1959).
[26] Lars Onsager, *Reciprocal Relations in Irreversible Processes. I.*, Phys. Rev. **37**, 405 (1931).
[27] G. L. Squires, *Introduction to the Theory of Thermal Neutron Scattering*, 3rd ed. (Cambridge University Press, Cambridge, England, 2012).
[28] M. Buttiker, *Symmetry of Electrical Conduction*, IBM J. Res. Dev. **32**, 317 (1988).
[29] S. W. Lovesey, *Theory of the Magnon and Phonon Interaction in* FeF_2, J. Phys. C **5**, 2769 (1972).
[30] G. Laurence and D. Petitgrand, *Thermal Conductivity and Magnon-Phonon Resonant Interaction in Antiferromagnetic* $FeCl_2$, Phys. Rev. B **8**, 2130 (1973).
[31] Lev Davidovich Landau and Evgenii Mikhailovich Lifshitz, *Quantum Mechanics: Non-relativistic Theory* (Elsevier, New York, 2013), Vol. 3.
[32] Léo Mangeolle, Leon Balents, and Lucile Savary, companion paper, *Thermal conductivity and theory of inelastic scattering of phonons by collective fluctuations*, Phys. Rev. B **106**, 245139 (2022).
[33] A linear term in magnon operators is generically present but does not contribute significantly to scattering due to phase-space constraints.
[34] T. Hahn, *Cuba—A Library for Multidimensional Numerical Integration*, Comput. Phys. Commun. **168**, 78 (2005).
[35] N. B. Christensen, H. M. Rønnow, D. F. McMorrow, A. Harrison, T. G. Perring, M. Enderle, R. Coldea, L. P. Regnault, and G. Aeppli, *Quantum Dynamics and Entanglement of Spins on a Square Lattice*, Proc. Natl. Acad. Sci. U.S.A. **104**, 15264 (2007).
[36] Bastien Dalla Piazza, M. Mourigal, Niels Bech Christensen, G. J. Nilsen, P. Tregenna-Piggott, T. G. Perring, Mechtild Enderle, Desmond Francis McMorrow, D. A. Ivanov, and Henrik Moodysson Rønnow, *Fractional Excitations in the Square-Lattice Quantum Antiferromagnet*, Nat. Phys. **11**, 62 (2015).
[37] H. M. Rønnow, D. F. McMorrow, R. Coldea, A. Harrison, I. D. Youngson, T. G. Perring, G. Aeppli, O. Syljuåsen, K. Lefmann, and C. Rischel, *Spin Dynamics of the 2D Spin* $\frac{1}{2}$ *Quantum Antiferromagnet Copper Deuteroformate Tetradeuterate (CFTD)*, Phys. Rev. Lett. **87**, 037202 (2001).
[38] Hiroshi Kameyama, Yoshihiro Ishibashi, and Yutaka Yakagi, *Elastic Constants in Cupric Formate Tetrahydrate Single Crystals*, J. Phys. Soc. Jpn. **35**, 1450 (1973).
[39] M. G. Cottam, *Spin-Phonon Interactions in a Heisenberg Antiferromagnet. II. The Phonon Spectrum and Spin-Lattice Relaxation Rate*, J. Phys. C **7**, 2919 (1974).
[40] Tao Qin, Jianhui Zhou, and Junren Shi, *Berry Curvature and the Phonon Hall Effect*, Phys. Rev. B **86**, 104305 (2012).
[41] Lifa Zhang, Jie Ren, Jian-Sheng Wang, and Baowen Li, *Topological Nature of the Phonon Hall Effect*, Phys. Rev. Lett. **105**, 225901 (2010).
[42] Yunchao Zhang, Yanting Teng, Rhine Samajdar, Subir Sachdev, and Mathias S. Scheurer, *Phonon Hall Viscosity from Phonon-Spinon Interactions*, Phys. Rev. B **104**, 035103 (2021).
[43] Mengxing Ye, Lucile Savary, and Leon Balents, *Phonon Hall Viscosity in Magnetic Insulators*, arXiv:2103.04223.
[44] Xiao-Qi Sun, Jing-Yuan Chen, and Steven A. Kivelson, *Large Extrinsic Phonon Thermal Hall Effect from Resonant Scattering*, Phys. Rev. B **106**, 144111 (2022).
[45] Haoyu Guo and Subir Sachdev, *Extrinsic Phonon Thermal Hall Transport from Hall Viscosity*, Phys. Rev. B **103**, 205115 (2021).
[46] Haoyu Guo, Darshan G. Joshi, and Subir Sachdev, *Resonant Thermal Hall Effect of Phonons Coupled to Dynamical Defects*, arXiv:2201.11681.
[47] Benedetta Flebus and A. H. MacDonald, *Charged Defects and Phonon Hall Effects in Ionic Crystals*, Phys. Rev. B **105**, L220301 (2022).
[48] Michiyasu Mori, Alexander Spencer-Smith, Oleg P. Sushkov, and Sadamichi Maekawa, *Origin of the Phonon Hall Effect in Rare-Earth Garnets*, Phys. Rev. Lett. **113**, 265901 (2014).